

Magnetic correlations in the Hubbard model on triangular and Kagomé lattices

N. Bulut^{1,2}, W. Koshibae¹ and S. Maekawa^{1,2}

¹*Institute for Materials Research, Tohoku University, Sendai 980-8577, Japan*

²*CREST, Japan Science and Technology Agency (JST), Kawaguchi, Saitama 332-0012, Japan*

(Dated: February 15, 2005)

In order to study the magnetic properties of frustrated metallic systems, we present Quantum Monte Carlo data on the magnetic susceptibility of the Hubbard model on triangular and Kagomé lattices. We show that the underlying lattice structure is important, and determines the nature and the doping dependence of the magnetic fluctuations. In particular, in the doped Kagomé case we find strong short-range magnetic correlations, which makes the metallic Kagomé systems a promising field for studies of superconductivity.

PACS numbers: 71.10.Fd, 71.10.Li, 74.70.-b, 74.25.Ha

Frustrated spin systems have received significant attention because of the possibility of novel magnetic ground-states and excitations [1]. The triangular spin-1/2 Heisenberg model has long-range magnetic order in the ground state, while the spin-1/2 Heisenberg model on the Kagomé lattice is considered to be disordered. The discovery of superconductivity at 5K in $\text{Na}_x\text{CoO}_2 \cdot y\text{H}_2\text{O}$ has generated new interest in frustrated interacting systems[2]. Furthermore, recently superconductivity has been discovered in β -pyrochlore osmate KOs_2O_6 with T_c of 10K [3]. This is interesting since the pyrochlore lattice structure is a three-dimensional analog of the Kagome lattice.

In cobaltates, cobalt and oxygen ions form a two-dimensional triangular network. The hopping matrix element of electrons in the cobalt 3d orbitals is not isotropic, and it has been shown that the triangular CoO_2 lattice consists of four coupled Kagomé sublattices [4]. Hence, it is important to compare the magnetic properties of interacting systems on triangular and Kagomé lattices. The electronic properties of the t - J and the Hubbard models on the triangular and Kagomé lattices have been studied using various techniques of many-body physics. The triangular t - J model was investigated within the RVB framework [5, 6, 7] and by using high-temperature expansions [8]. The triangular Hubbard model was studied with the path-integral renormalization-group (RG) [9], the one-loop RG [10] and the fluctuation-exchange (FLEX) [11] approaches. The FLEX method was also used for studying the magnetic properties of the Hubbard model on the Kagomé lattice [12].

In this paper, we compare the nature of the magnetic correlations in the Hubbard model on the triangular and the Kagomé lattices using Quantum Monte Carlo (QMC) simulations. We consider the Hubbard model on the Kagomé lattice to be a simple limiting case to explore for new physics due to the underlying orbital structure in frustrated interacting systems. The orbital degrees of freedom create the possibility for mixing the spin and charge channels, and hence of new electronic states. This is important because of the general ongoing research ef-

fort on the transition metal oxides. These are our motivations for performing the QMC calculations on the Hubbard model on the triangular and the Kagomé lattices. We are particularly interested in the doped cases of these models for which there are no exact calculations on the magnetic properties.

In the following, we will see that the nature of the magnetic fluctuations on the triangular and the Kagomé lattices are different. For the triangular lattice, the QMC results show that there are strong antiferromagnetic (AF) correlations near half-filling at low temperatures, when the Coulomb repulsion U is of the order of the bandwidth. On the other hand, for weak U , the magnetic correlations saturate as $T \rightarrow 0$. In the Kagomé lattice, the unit cell consists of three atoms and the unit cells form a triangular lattice, as seen in Fig. 1(a). Consequently, there are three bands of magnetic excitations. Two of these modes involve enhanced short-range AF correlations. We find that, in the doped Kagomé case, the low-frequency short-range AF correlations are stronger in comparison to the triangular lattice. Hence, we note that it would be useful to investigate the possibility of superconductivity in metallic Kagomé systems.

The Hubbard model is defined by

$$H = -t \sum_{\langle i,j \rangle, \sigma} (c_{i\sigma}^\dagger c_{j\sigma} + \text{h.c.}) + U \sum_i n_{i\uparrow} n_{i\downarrow} - \mu \sum_{i\sigma} n_{i\sigma}, \quad (1)$$

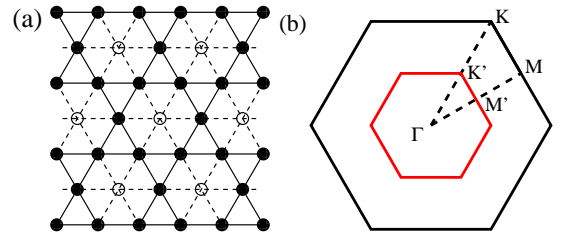


FIG. 1: (a) Sketch of the triangular and the Kagomé lattices. The Kagomé lattice is obtained from the triangular lattice by removing the sites with the open circles. (b) First Brillouin zones of the triangular (black) and the Kagomé (red) lattices.

where t is the hopping matrix element between the nearest neighbor-sites, U is the on-site Coulomb repulsion, and μ is the chemical potential. Here, $c_{i\sigma}$ ($c_{i\sigma}^\dagger$) annihilates (creates) an electron with spin σ at site i , and $n_{i\sigma} = c_{i\sigma}^\dagger c_{i\sigma}$. In the following, we will take $t < 0$ and consider $\langle n \rangle \geq 1.0$, which is the appropriate case for the cobaltates [4]. In obtaining the QMC data presented here, the determinantal QMC technique [13] was used.

For the triangular lattice, the longitudinal magnetic susceptibility at frequency $\omega = 0$ is defined by

$$\chi(\mathbf{q}) = \int_0^\beta d\tau \sum_\ell e^{-i\mathbf{q}\cdot\mathbf{r}_\ell} \langle m^z(\mathbf{r}_{i+\ell}, \tau) m^z(\mathbf{r}_i) \rangle, \quad (2)$$

where $m^z(\mathbf{r}_i) = c_{i\uparrow}^\dagger c_{i\uparrow} - c_{i\downarrow}^\dagger c_{i\downarrow}$ and $m^z(\mathbf{r}_i, \tau) = e^{H\tau} m^z(\mathbf{r}_i) e^{-H\tau}$. In this paper, results on χ will be shown in units of $|t|^{-1}$.

The Kagomé lattice is a three-band model, since each unit cell consists of three sites. Hence, each lattice on the Kagomé lattice site can be represented by the indices (ℓ, d) where ℓ is the unit-cell index and d denotes the atomic site in a particular unit cell. The corresponding Brillouin zone (BZ) is reduced with respect to the triangular case as illustrated in Fig. 1(b). For the Kagomé case, we define the longitudinal magnetic susceptibility at $\omega = 0$ as

$$\chi_{dd'}(\mathbf{q}) = \int_0^\beta d\tau \sum_\ell e^{-i\mathbf{q}\cdot\mathbf{r}_\ell} \langle m_d^z(\mathbf{r}_{i+\ell}, \tau) m_{d'}^z(\mathbf{r}_i) \rangle, \quad (3)$$

where $m_d^z(\mathbf{r}_i) = c_{i\uparrow}^\dagger c_{i\uparrow} - c_{i\downarrow}^\dagger c_{i\downarrow}$, $c_{i\downarrow}$ ($c_{i\downarrow}^\dagger$) is the annihilation (creation) operator of an electron with spin σ at lattice site (i, d) and the summation is performed over the unit-cell locations. Diagonalizing the 3×3 matrix $\chi_{dd'}(\mathbf{q})$, we obtain $\chi_\alpha(\mathbf{q})$ which describes the three modes of the magnetic excitations on the Kagomé lattice, which we define as the Kagomé magnetic bands. At this point, it is useful to note that already for the noninteracting ($U = 0$) case, the triangular and the Kagomé lattices have different properties. For $t < 0$, the one-electron density of states $N(\omega)$ of the triangular lattice has a van Hove singularity at $\langle n \rangle = 0.5$. For the Kagomé lattice, there is a δ -function singularity in $N(\omega)$ at the bottom of the band and there are van Hove singularities at $\langle n \rangle = 1.16$ and 1.51 . In addition, $N(\omega = 0)$ vanishes at $\langle n \rangle = 1.33$. These features of $N(\omega)$ are also reflected in the magnetic susceptibilities of the noninteracting case.

We first present results for the triangular lattice at half-filling. Figure 2(a) shows $\chi(\mathbf{q})$ versus \mathbf{q} for $U = 4|t|$ on various size lattices as the temperature is lowered. Here, it is seen that $\chi(\mathbf{q})$ has a broad peak centered at the K point of the BZ, and hence the system exhibits short-range AF correlations. We also note that $\chi(\mathbf{q})$ does not vary significantly with T , in particular for $0.25|t| \leq T \leq 0.17|t|$. For comparison, $\chi_0(\mathbf{q})$ for the noninteracting system at $T = 0.17|t|$ is shown by the dotted

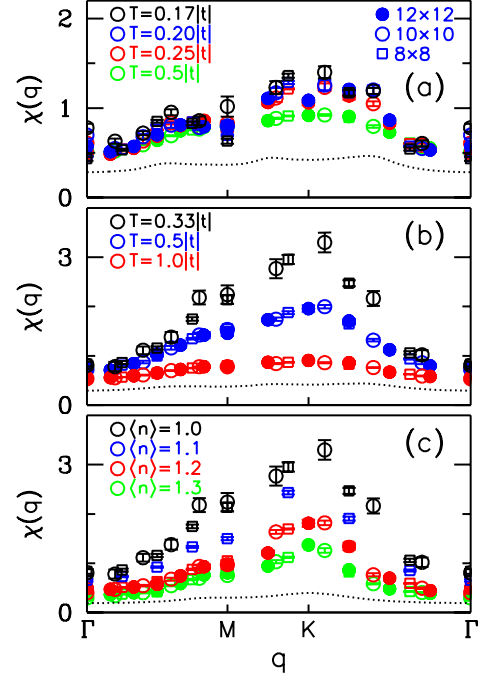


FIG. 2: Magnetic susceptibility $\chi(\mathbf{q})$ versus \mathbf{q} of the triangular Hubbard model at zero frequency. Here, \mathbf{q} is scanned along the path $\Gamma \rightarrow M \rightarrow K \rightarrow \Gamma$ in the BZ of the triangular lattice illustrated in Fig. 1(b). The temperature evolution of $\chi(\mathbf{q})$ at half-filling is shown in (a) for $U = 4|t|$ and in (b) for $U = 8|t|$. In these figures, the dotted curves represent results for the noninteracting case at the lowest temperature used in that figure. The evolution of $\chi(\mathbf{q})$ versus \mathbf{q} with the electron density $\langle n \rangle$ is shown in (c) for $U = 8|t|$ and $T = 0.33|t|$. Here, the dotted curve represents the results for the noninteracting system at $\langle n \rangle = 1.3$ and $T = 0.33|t|$.

curve. Figure 2(b) displays $\chi(\mathbf{q})$ versus \mathbf{q} for $U = 8|t|$ at half-filling, where we observe a large Stoner enhancement of the AF correlations. In contrast with the $U = 4|t|$ case, here, $\chi(\mathbf{q})$ at the K point grows rapidly with a Curie-like T dependence, as T decreases from $1|t|$ to $0.33|t|$. However, it is not known whether $\chi(\mathbf{q})$ saturates at lower T for $U = 8|t|$. These results show that the T dependence of $\chi(\mathbf{q})$ depends strongly on the value of $U/|t|$ in the triangular Hubbard model, in agreement with the findings of the path-integral RG calculations [9].

Figure 2(c) shows the filling dependence of $\chi(\mathbf{q})$ for $U = 8|t|$ while T is kept fixed at $0.33|t|$. Here, we observe that the AF correlations decay monotonically as the electron filling is varied from 1.0 to 1.3. We have also performed calculations for $\chi(\mathbf{q})$ at higher electron fillings. We find that, when $\langle n \rangle$ is increased to 1.5, the peak in $\chi(\mathbf{q})$ shifts to the M point. Upon further doping to $\langle n \rangle = 1.75$, we find that, for $U = 8|t|$ and $T = 0.2|t|$, the Stoner enhancement is about 20%. Hence, for this dilute hole concentration, the magnetic correlations are weakly affected by the presence of the on-site Coulomb

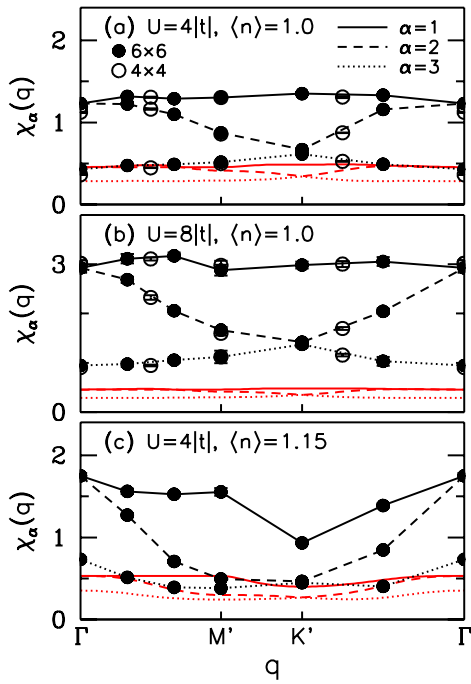


FIG. 3: Magnetic susceptibility $\chi_\alpha(\mathbf{q})$ versus \mathbf{q} for the Hubbard model on the Kagomé lattice at zero frequency. Here, the three magnetic modes of $\chi_\alpha(\mathbf{q})$ are shown at each \mathbf{q} point, as \mathbf{q} is scanned along the path $\Gamma \rightarrow M' \rightarrow K' \rightarrow \Gamma$ in the first BZ of the Kagomé lattice illustrated in Fig. 1(b). Results on $\chi_\alpha(\mathbf{q})$ at half-filling are shown in (a) for $U = 4|t|$ and $T = 0.2|t|$ and in (b) for $U = 8|t|$ and $T = 0.33|t|$. These data have been obtained on lattices with 6×6 and 4×4 unit cells. In (c), results are shown for $\langle n \rangle = 1.15$ with $U = 4|t|$ and $T = 0.14|t|$. In these figures, the data points for the 6×6 lattice are connected by black lines, and the red curves represent the results for the noninteracting case.

repulsion at this temperature. For $U = 4|t|$, $\chi(\mathbf{q})$ exhibits a slow monotonic decrease with the electron doping away from half-filling.

Next, we discuss the magnetic properties of the Hubbard model on the Kagomé lattice. Figure 3(a) shows QMC results on $\chi_\alpha(\mathbf{q})$ for $U = 4|t|$ and $T = 0.2|t|$ at half-filling. Here, $\chi_\alpha(\mathbf{q})$ for the three magnetic bands are plotted as a function of \mathbf{q} , and the red curves represent results for the noninteracting case. In this figure, we observe that the top band ($\alpha = 1$) is flat in \mathbf{q} space, and the second magnetic band ($\alpha = 2$) is degenerate with the first one at the zone center. The third mode is weaker in magnitude and exhibits a smooth \mathbf{q} dependence. Figure 3(b) shows $\chi_\alpha(\mathbf{q})$ versus \mathbf{q} for $U = 8|t|$ and $T = 0.33|t|$ at half-filling. The general features are similar to those seen in Fig. 3(a), however here the Stoner enhancement is larger. In Fig. 3(c), the QMC results are shown for $U = 4|t|$ and $T = 0.14|t|$ at $\langle n \rangle = 1.15$. These figures show that the features of $\chi_\alpha(\mathbf{q})$ are in correspondence with those of the noninteracting case.

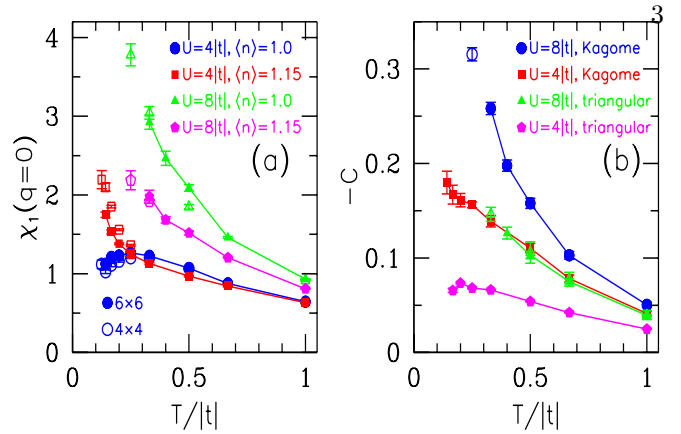


FIG. 4: (a) $\chi_1(\mathbf{q} = 0)$ versus T for the Kagomé lattice with $U = 4|t|$ and $8|t|$ at $\langle n \rangle = 1.0$ and 1.15 . (b) Zero-frequency component of the magnetic correlations between the nearest-neighbor sites C versus T for the Kagomé and the triangular lattices at $\langle n \rangle = 1.15$ for $U = 8|t|$ and $4|t|$. In these figures, the results on the Kagomé lattice were obtained for 6×6 (solid points) and 4×4 (open points) unit cells, and the results on the triangular lattice are for 12×12 (solid points) and 8×8 (empty points) lattices. In addition, the data points for the 6×6 Kagomé and the 12×12 triangular lattices have been connected by solid lines.

In order to gain insight into the origin of the Kagomé magnetic bands, we note that the Kagomé lattice is obtained from the triangular lattice, as illustrated in Fig. 1(a), by removing the sites with the empty circles. This is equivalent to putting an infinitely repulsive one-electron potential at these sites. Bragg scattering from this static charge-density-wave field then folds the BZ of the triangular lattice, and also mixes the different wavevector components of the spin fluctuations. It is this process which creates the Kagomé magnetic bands.

We next discuss the T dependence of the magnetic correlations in the Kagomé lattice. Figure 4(a) shows $\chi_1(\mathbf{q} = 0)$ versus T for $U = 4|t|$ and $8|t|$ at $\langle n \rangle = 1.0$ and 1.15 . Here, we observe that, at half-filling and for $U = 4|t|$, $\chi_1(\mathbf{q} = 0)$ saturates as T decreases. On the other hand, for $U = 8|t|$, $\chi_1(\mathbf{q} = 0)$ has a strong T -dependence. For $\langle n \rangle = 1.15$ and $U = 4|t|$, we observe that $\chi_1(\mathbf{q} = 0)$ gets enhanced at low T , and becomes larger than at half-filling. We also see that the enhancement of $\chi_1(\mathbf{q} = 0)$ depends on the lattice size. However, this type of non-monotonic doping dependence was not observed for the triangular Hubbard model. In addition, we observe that, for $U = 8|t|$ and at half-filling, $\chi_1(\mathbf{q} = 0)$ exhibits a Curie-like T dependence for $0.25|t| \leq T \leq 1.0|t|$. In the ground state of the Heisenberg model on the Kagomé lattice, it is considered that a spin gap $\Delta_S \approx J/20$ exists, where J is the magnetic exchange [1]. For $U = 8|t|$, we have $J \approx 4t^2/U = 0.5|t|$, which gives $\Delta_S \approx 0.025|t|$. We expect that $\chi_\alpha(\mathbf{q})$ saturates before T becomes comparable to Δ_S . However, already at $T = 0.33|t|$ we observe enhanced magnetic

correlations.

The FLEX calculations for the Hubbard model on the Kagomé lattice find that the leading magnetic mode is nearly \mathbf{q} independent, and the tendency to electronic instabilities is suppressed [12]. We note that while the $\alpha = 1$ mode is nearly \mathbf{q} independent, the $\alpha = 2$ mode has ferromagnetic \mathbf{q} dependence in the sense that it decreases away from the Γ point. In addition, the eigenvectors of $\chi_{dd'}(\mathbf{q})$ show that, at $\mathbf{q} \approx 0$, the $\alpha = 1$ and 2 modes describe excitations involving the AF polarization of the spins within a unit cell [14]. Away from $\mathbf{q} = 0$, these modes have additional structures, however they involve AF polarizations over most of the BZ. Hence, these two modes contain enhanced short-range AF fluctuations. Within the context of superconductivity mediated by magnetic fluctuations, an important quantity is the zero-frequency component of the magnetic fluctuations between the two nearest-neighbor sites i and j ,

$$C = \int_0^\beta d\tau \langle m^z(\mathbf{r}_i, \tau) m^z(\mathbf{r}_j) \rangle. \quad (4)$$

In Fig. 4(b), we compare C versus T for the triangular and the Kagomé lattices for $U = 4|t|$ and $8|t|$ at $\langle n \rangle = 1.15$. This figure shows that, at these temperatures, the nearest-neighbor AF correlations are stronger for the Kagomé lattice, even though the ground-state of the spin-1/2 Heisenberg model has long-range order on the triangular lattice and it is disordered in the Kagomé case. Hence, it would be useful to investigate the possibility of superconductivity in metallic Kagomé systems.

Finally, we discuss the implications of these data for the magnetic correlations observed in the cobaltates. The cobaltates have a rich phase diagram with superconductivity found for $x \approx 0.35$ in $\text{Na}_x\text{CoO}_2 \cdot y\text{H}_2\text{O}$ [2] and with magnetic order and large quasi-particle renormalizations observed in Na_xCoO_2 when x is near 0.75 [15]. For the triangular Hubbard model, we find that the magnetic correlations are strongest at half-filling, and the correlation effects are weak in the overdoped regime $\langle n \rangle \geq 1.5$. In contrast, for the Kagomé lattice we have seen that the magnetic correlations can be stronger in the doped case when $U = 4|t|$. However, in both of these models, we find that the correlation effects are most prominent in the vicinity of half-filling at the temperatures where the QMC calculations were performed. We note that it would be useful to determine experimentally the \mathbf{q} dependence of the magnetic fluctuations in the superconducting $\text{Na}_x\text{CoO}_2 \cdot y\text{H}_2\text{O}$.

In this paper, we have investigated the nature of the magnetic correlations in the Hubbard model on the triangular and Kagomé lattices. At the temperatures where the QMC calculations were performed, we find, in both of these models, that the magnetic correlations grow rapidly as T decreases at half-filling for $U = 8|t|$, while they sat-

urate when $U = 4|t|$. In the triangular Hubbard model, the AF correlations decay monotonically with the electron doping. In the Kagomé case, on the other hand, we have seen that the magnetic correlations can be stronger in the doped case when $U = 4|t|$. We have also seen that in the Kagomé case the BZ is reduced and there are three modes of magnetic excitations. The two leading modes involve short-range AF correlations. In particular, we find that the low-frequency short-range AF correlations are stronger in the doped Kagomé case than in the triangular case. This makes the interacting metallic systems with Kagomé type of lattice structures a promising field for studies of superconductivity. We conclude that in frustrated interacting systems the underlying lattice and orbital structures are important in determining the magnetic properties.

The authors are grateful to Y.Y. Bang, C. Honerkamp, M. Imada, K. Ishida, S. Ishihara, T. Koretsune, P. Lee, Y. Motome, B. Normand, T.M. Rice, T. Tohyama and G.-q. Zheng for helpful discussions. One of us (N.B.) would like to thank the International Frontier Center for Advanced Materials at Tohoku University for its kind hospitality, and gratefully acknowledges partial support from the Turkish Academy of Sciences through the GEBIP program (EA-TUBA-GEBIP/2001-1-1). This work was supported by Priority-Areas Grants from the Ministry of Education, Science, Culture and Sport of Japan, NAREGI Japan and NEDO.

-
- [1] G. Misguich and C. Lhuillier, *"Frustrated spin systems"*, Ed. H.T. Diep, World-Scientific (2004), and references therein.
 - [2] K. Takada *et al.*, Nature (London) **422**, 53 (2003).
 - [3] S. Yonezawa *et al.*, J. Phys.: Cond. Mat. **16**, L9 (2004).
 - [4] W. Koshibae and S. Maekawa, Phys. Rev. Lett. **91**, 257003 (2003).
 - [5] G. Baskaran, Phys. Rev. Lett. **91**, 097003 (2003).
 - [6] B. Kumar and B. S. Shastry, Phys. Rev. B **68**, 104508 (2003).
 - [7] Q.-H. Wang, D.-H. Lee and P.A. Lee, Phys. Rev. B **69**, 092504 (2004).
 - [8] T. Koretsune and M. Ogata, Phys. Rev. Lett. **89**, 116401 (2002).
 - [9] T. Kashima and M. Imada, J. Phys. Soc. Jpn. **70**, 3052 (2001).
 - [10] C. Honerkamp, Phys. Rev. B **68**, 104510 (2003).
 - [11] M. Renner and W. Brenig, cond-mat/0310244.
 - [12] Y. Imai, N. Kawakami and H. Tsunetsugu, Phys. Rev. B **68**, 195103 (2003).
 - [13] S.R. White *et al.*, Phys. Rev. B **40**, 506 (1989).
 - [14] We also note that, at $\mathbf{q} \approx 0$, the $\alpha = 3$ mode corresponds to fluctuations involving the uniform polarization of the spins within a unit cell, and hence the Knight shift for the Kagomé lattice is determined by $\chi_3(\mathbf{q} \rightarrow 0)$.
 - [15] M.L. Foo *et al.*, Phys. Rev. Lett. **92**, 247001 (2004).